A Copolymer of Monomethoxy Poly(ethylene glycol)-Polycaprolactone as Form-Stable Phase Change Materials for Thermal Energy Storage

Pin Jin Ong,[a] Hui Yi Shuko Lee,[a] Dr. Jayven Chee Chuan Yeo,[a] Dr. Zibiao Li,[a, b, d] Dr. Johnathan Joo Cheng Lee,[a] Dr. Suxi Wang,[a] Dr. Xuesong Yin,[a] Dr. Pei Wang,[a] Dr. Jianwei Xu,[a, b, c] Prof. Xian Jun Loh,[a, b, d] Dr. Joseph Kinyanjui Muiruri,*[b] and Dr. Qiang Zhu *[a, b, e]

[a] Institute of Materials Research and Engineering (IMRE), Agency for Science, Technology and Research (A*STAR), 2 Fusionopolis Way, Innovis #08-03, Singapore 138634
[b] Institute of Sustainability for Chemicals, Energy and Environment (ISCE^2), Agency for Science, Technology and Research (A*STAR), 1 Pesek Road, Jurong Island, Singapore 627833
[c] Department of Chemistry, National University of Singapore, 3 Science Drive 3, Singapore 117543
[d] Department of Material Science and Engineering, National University of Singapore, 9 Engineering Drive 1, #03-09 EA, Singapore 117575
[e] School of Chemistry, Chemical Engineering and Biotechnology, Nanyang Technological University, 21 Nanyang Link, Singapore 637371

Corresponding email: joseph_muiruri@isce2.a-star.edu.sg; zhuq@imre.a-star.edu.sg

Abstract

In this work, a series of monomethoxy poly(ethylene glycol)-polycaprolactone (mPEG-PCL) copolymers with different mass percentages of mPEG was chemically synthesized as form-stable phase change materials (FSPCMs) for thermal energy storage (TES) application for the first time. Their chemical structures, surface morphology, and thermal properties were studied in terms of nuclear magnetic resonance (NMR), Fourier transform infrared spectroscopy (FTIR), scanning electron microscopy (SEM), thermogravimetric analysis (TGA), and differential scanning calorimetry (DSC). ^{1}H NMR, gel permeation chromatography (GPC), and FTIR results confirmed the successful ring-opening polymerization of ε-caprolactone with mPEG macromonomer, and the respective average molecular weight of the copolymers was obtained in the range of 9704-17346 g mol^{-1}. DSC analysis results revealed that the copolymers have a phase change temperature and latent heat in the range of 52.8-57.9 °C and 88.8-114.4 J g^{-1} respectively and TGA analysis showed that they are thermally stable up to 150 °C. Leakage test results showed that the copolymers $(mPEG)_x$-$(PCL)_y$ displayed excellent form stability with minimal leakage while thermal cycling revealed good thermal reliability. In addition, the copolymers successfully demonstrated their ability to store and release heat for a prolonged period, making them suitable for TES applications like heating water storage tanks.

Introduction

Due to the rising energy crisis, shortage in fossil fuel reserves, and increase in greenhouse gas emissions over the past two decades, a myriad of energy storage technologies have since been studied and developed extensively by researchers.[1-3] Latent heat thermal energy storage (LHTES) systems using phase change materials (PCMs) have been drawing great attention due to their small temperature fluctuations and high energy storage density. It endows them with the ability to store and release large amounts of energy during the phase change process without changing their properties, unlike phase transformation processes.[4-8] Therefore, such technologies have been broadly applied in buildings,[9-10] electronics,[11] solar energy utilization,[12] thermoelectric materials,[13-15] and textiles.[16]

Based on their phase transition type, PCMs fall into four categories: solid-solid PCMs (SSPCMs), solid-liquid PCMs (SLPCMs), solid-gas PCMs (SGPCMs), and liquid-gas PCMs (LGPCMs).[17-18] In general, SGPCMs and LGPCMs exhibit higher latent heat storage capacities compared to the other two types but they are not for practical use due to large volumetric changes during the phase change process. For SSPCMs, even though they experience small volume changes, and no container is required to seal them, their small latent heat capacity and super-cooling issue restrict their applications.[19-20] SLPCMs, on the other hand, have been studied and applied extensively in LHTES systems due to their outstanding properties such as high latent thermal storage capacity, non-corrosiveness, good thermal and chemical stability, non-toxicity, small volume change during the phase transition, little or no super-cooling and so on.[21-23] However, in comparison to SSPCMs, the major shortcoming of SLPCMs is the leakage issue during the phase transition, which limits their direct application.[24-25] Therefore, they have to be placed in special containers to circumvent this problem.[26]

Among the investigated SLPCMs, monomethoxy poly(ethylene glycol) (mPEG) and poly(ethylene glycol) (PEG) have been considered promising PCMs for TES because of their low thermal hysteresis, relatively high latent heat, wide melting point range, high chemical and thermal stability, non-corrosiveness and non-toxicity.[27-28] In addition, they can be physically or chemically modified easily due to the presence of hydroxy end groups. Therefore, to address the leakage issue, PEG-based form-stable PCMs (FSPCMs) have been studied extensively in recent years.[29-31]

In general, FSPCMs are mainly composed of SLPCMs and supporting materials (usually polymers with high melting temperatures [32-33] or inorganic materials with lamellar/porous structure [34-36]), which can maintain a solid form with no leakage at ambient temperatures higher than the phase transition temperature. PEG-based FSPCMs can be prepared by physically embedding PEG into porous supporting materials, such as graphene oxide,[37] epoxy resin,[38] diatomite,[39] and expanded graphite.[40] However, these materials might be costly and possess low porosity and such FSPCMs are prone to instability in solvents. On the other hand, the stability of PEG-based FSPCMs can be improved via chemical modification methods, such as grafting or cross-linking with polymeric materials. For example, Liu et al. [41] prepared a semi-interpenetrating polymer network consisting of PEG and poly(polyethylene glycol diacrylate as a supporting material via in-situ polymerization as a FSPCM. Alva et al. [42] prepared PEG-based polyurethane (PU) copolymers using branching and linear chain extension methods, where 4,4'Diphenylmethane di-isocyanate served as a cross-linked and chain extender. Kong et al. [43] developed a series of cross-linked PEG and PU blends, where PU functioned as both the phase change substance and supporting material. Tan et al. [44] prepared a vesicle-like structure FSPCM via an in-situ polyaddition reaction between a carboxylic acid terminated PEG and trimethylolpropane tris (2-methyl-1-aziridine propionate (TMPTAP), where PEG served as a self-template to regulate the gel network structure.

It is known that wet chemistry can be used to synthesize different functional molecules.[45-47] Poly(caprolactone) (PCL) is a biodegradable polyester with a low melting point and is synthesized with ε-caprolactone using the ring-opening polymerization method. Its application in the medical industry has been extensively ranging from surgical implants to drug delivery devices in regenerative medicine.[48-50] However, the drawbacks of PCL are their low melting point and low glass transition

temperature which limits their application at higher temperatures.[51] Therefore, PCL is usually mixed with other polymers such as PEG to produce composites with desired properties.

The synthesis of mPEG-PCL grafted copolymers can be carried out by ring-opening polymerization of ε-caprolactone on the hydroxy site of the mPEG macromonomer and it proceeds via an environmentally friendly route that is easily replicable with an active transesterification catalyst.[52] Therefore, mPEG-PCL copolymers can be polymerized in bulk for applications in different areas such as in drug delivery,[53] soft tissue engineering,[54] and surgical application.[55] The mPEG-PCL copolymer has also demonstrated greater compatibility when compared to non-modified PEG.[56]

In this study, a series of mPEG-PCL copolymers with different mass percentages of mPEG were synthesized for TES applications. The effect of mPEG mass content on the structure, thermal and chemical stability, and form stability was analyzed using various techniques. In addition, a leakage test was conducted to evaluate their form stability, and the performance of one of the copolymers for an application demonstrating the heating of water storage tanks was examined.

Materials and methods

Materials

ε-caprolactone, monomethoxy poly(ethylene glycol) (M_n = 5000 Da), tin octanoate, and diethyl ether were purchased from Sigma Aldrich unless otherwise stated. Purasorb L (L-lactide) was obtained from Corbion while toluene & chloroform were purchased from Fluka.

Synthesis of copolymers $(mPEG)_x$-$(PCL)_y$

The synthesis route is shown in Figure 1 and the different composition ratios of the copolymers are shown in Table 1. Copolymers prepared from mPEG and PCL are designated as $(mPEG)_x$-$(PCL)_y$, where the ratios of x to y are 2:1, 1:1, and 1:2.

The synthesis of $(mPEG)_2$-$(PCL)_1$ was carried out by weighing 5 g of mPEG (5k) and 2.5 g of ε-caprolactone. In a three-neck flask, the weighed mPEG and ε-caprolactone were dissolved in 60 mL of toluene. 30 mg of tin octanoate (stannous 2-ethylhexanoate) was added and the mixture is left to be refluxed at 120 °C under a nitrogen atmosphere for 24 h. After 24 h, an adequate amount of chloroform was added to the resultant product to dissolve. After that, the mixture was vigorously stirred, precipitated in diethyl ether at 0 °C, and filtered. The precipitated polymer was left to be dried at room temperature, then in a vacuum oven at 60 °C. The obtained copolymer product has a white or off-white powder appearance.

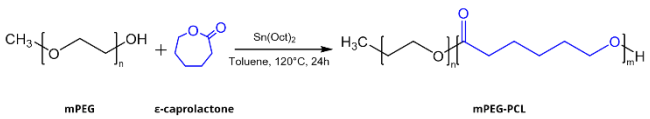

Fig. 1. Synthetic route for copolymers $(mPEG)_x$-$(PCL)_y$ via ring-opening polymerization.

Table 1. Composition ratio for copolymers $(mPEG)_x$-$(PCL)_y$.

Sample	Feed ratio	Monomer 1 (macroinitiator)	Monomer 2	Catalyst	Solvent
$(mPEG)_2$-$(PCL)_1$	2:1	5 g mPEG (5k)	2.5 g ε-caprolactone	30 mg Tin octanoate	60 mL Toluene

$(mPEG)_1$-$(PCL)_1$	1:1	5 g mPEG (5k)	5.0 g ε-caprolactone	30 mg Tin octanoate	60 mL Toluene
$(mPEG)_1$-$(PCL)_2$	1:2	5 g mPEG (5k)	10.0 g ε-caprolactone	30 mg Tin octanoate	60 mL Toluene

NMR analysis of copolymers $(mPEG)_x$-$(PCL)_y$

The synthesized $(mPEG)_x$-$(PCL)_y$ copolymers were analyzed using ^1H NMR (JEOL 500 MHz NMR spectrometer) in deuterated chloroform ($CDCl_3$).

GPC analysis of copolymers $(mPEG)_x$-$(PCL)_y$

Gel permeation chromatography (GPC) was analyzed using an Agilent 1260 Infinity II GPC/SEC System. HPLC-grade tetrahydrofuran (THF) as eluent was used, with a flow rate of 1.0 mL min^{-1} at 40 ºC. The calibration curve was obtained using monodispersed poly(styrene) standards.

FTIR analysis of copolymers $(mPEG)_x$-$(PCL)_y$

The structure of the copolymers was analyzed using a Spectrum 2000 Fourier Transform Infrared Spectroscopy (FTIR) instrument (PerkinElmer). Each copolymer sample was tested using 16 scans with a spectrum resolution of 4 cm^{-1}, over the frequency range of 4000 and 400 cm^{-1}.

SEM analysis of copolymers $(mPEG)_x$-$(PCL)_y$

The morphological study of the copolymers was performed using JEOL JSM6700F scanning electron microscope (SEM). The samples were coated with a thin layer of gold using sputter coating and the micrographs were taken in a high vacuum mode with 10 µA emission current and 5 kV acceleration voltage.

Thermophysical properties of copolymers $(mPEG)_x$-$(PCL)_y$

The thermal stability of the $(mPEG)_x$-$(PCL)_y$ copolymers was evaluated with the thermogravimetric analyzer (Q500, TA Instruments, USA). The copolymers were heated from 25 °C to 800 °C at a rate of 20 °C min^{-1} under a nitrogen atmosphere at a flow rate of 60 mL min^{-1}. The phase transition temperature and latent heat of the $(mPEG)_x$-$(PCL)_y$ copolymers were measured using a differential scanning calorimeter (Q100, TA instruments, USA), with nitrogen gas at a flow rate of 50 mL min^{-1}. Each copolymer sample was loaded into an aluminum hermetic pan and measured from -25 °C to 80 °C at a heating and cooling rate of 5 °C min^{-1}. To determine the thermal reliability of the copolymer, 100 melt/freeze cycles were conducted using the same equipment and gas flow as mentioned above for determining the phase transition temperature. They were heated from -10 °C to 80 °C at a rate of 20 °C/min and held for 1 min. The samples were cooled from 80 °C to -10 °C using the same rate of 20 °C/min and held for 1 min. The entire process was repeated 99 times.

Form stability and leakage test

The form stability of copolymers $(mPEG)_x$-$(PCL)_y$ was evaluated by conducting a leakage test. 0.3 g of each of the three $(mPEG)_x$-$(PCL)_y$ copolymers was made into a pellet by pressing it at 10 ton for 2 min using a manual hydraulic press (Specac). Each pellet has a diameter of 1.3 cm and thickness of 2 mm and the initial mass (M_0) of each sample was measured. The samples were each placed on a filter paper in a petri dish and put in the oven at 75 °C for 4 h. The samples were taken out from the oven and allowed to cool before measuring the weight (M_n) at intervals of 1 h. Images of the samples before and after the leakage test were taken and the leakage rate (L) was calculated as per Equation (1):

$$L = (M_0 - M_n) / M_0 \times 100\% \quad (1)$$

TES performance test

A stainless-steel pipe (length: 20 cm, outer diameter: 1.5 cm) was placed within another stainless-steel pipe (length: 6 cm, inner diameter: 2.1 cm), with both ends of the outer pipe having a distance of 7 cm away from both ends of the inner pipes. The gap between both pipes at the bottom was sealed. 15 g of $(mPEG)_2$-$(PCL)_1$ was prepared and poured into the gap at the top and left to cool at room temperature. The outer pipe was removed, and the resulting sample formed on the inner pipe has a length of 5.5 cm and a thickness of 0.3 cm. The pipe was then secured to two retort stands and connected to a water circulator as shown in Figure 2. An infrared red (IR) camera (FLIR A65) was used for capturing the IR images and monitoring the temperature changes. The water circulator was set to 80 ℃ and left to run for 15 min and subsequently set to 25 ℃. IR images of the stainless-steel pipe with the sample were taken at regular intervals until the sample was completely cooled.

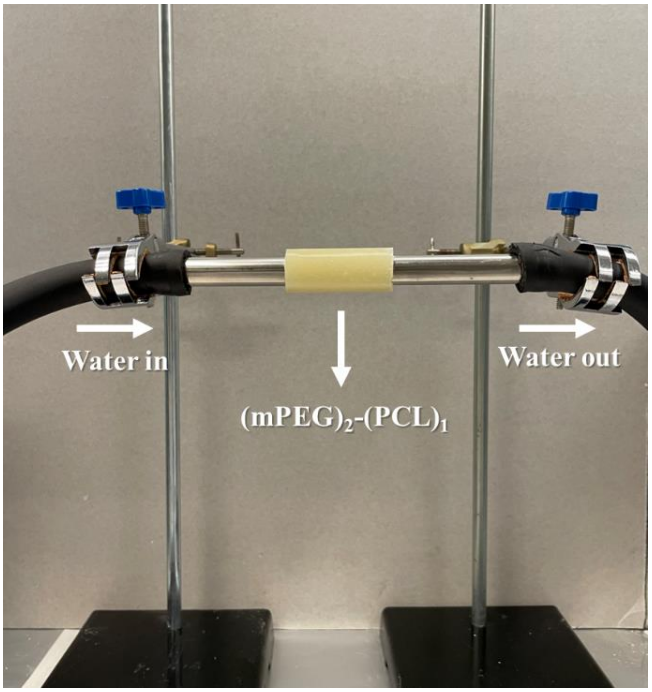

Fig. 2. Experimental set-up of application study with $(mPEG)_2$-$(PCL)_1$.

Results and discussion

NMR and GPC analysis of copolymers $(mPEG)_x$-$(PCL)_y$

^{1}H-NMR spectra of $(mPEG)_x$-$(PCL)_y$ copolymers presented in Figure 3 confirmed the successful grafting of mPEG onto PCL. The singlet peak at around 3.6-3.7 ppm corresponds to the methylene protons (–CH_2–) present at the mPEG monomer (peaks a,b) as there are no neighboring carbons with hydrogen attached. The triplet peak at around 2.2-2.4 ppm is attributed to the methylene protons (–CH_2–) next to the ester functional group (–COO–) of the mPEG monomer (peak c) while the peaks between 1.3-1.7 ppm are due to the methylene protons in the PCL chains (peaks d-f). The triplet peak between 4.0-4.1 ppm is assigned to PCL's methoxy group (–CH_2–O–) (peak g).

GPC is the commonly used technique for the determination of polymer molecular weight. By employing GPC, we determined the molecular weights and the degree of polymerization (Fig. S1) of mPEG (DP_{mPEG}) and PCL (DP_{PCL}) of the resultant samples as seen in Table 2. As seen in Table 2, the M_n values obtained for $(mPEG)_2$-$(PCL)_1$, $(mPEG)_1$-$(PCL)_1$, and $(mPEG)_1$-$(PCL)_2$ copolymers are 9704, 10799,

and 17346 g/mol, respectively. Clearly, the M_n and M_w values reveal that the GPC chromatogram of copolymers is monomodal but with wide molecular weight distribution as depicted by their polydispersity (PDI, M_w/M_n).[57]

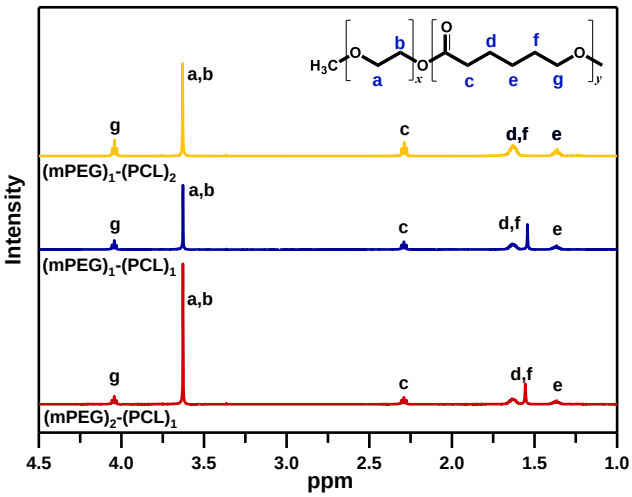

Fig. 3. ^{1}H NMR of copolymers $(mPEG)_1$-$(PCL)_2$, $(mPEG)_1$-$(PCL)_1$ and $(mPEG)_2$-$(PCL)_1$.

Table 2. Molecular characterization of copolymers $(mPEG)_x$-$(PCL)_y$.

Sample	M_n	M_w	PDI	DP_{PCL}	DP_{mPEG}
$(mPEG)_2$-$(PCL)_1$	9700	12500	1.29	51	152
$(mPEG)_1$-$(PCL)_1$	10800	14700	1.36	93	93
$(mPEG)_1$-$(PCL)_2$	17300	25700	1.48	115	287

FTIR analysis

The FTIR spectra of mPEG and copolymers $(mPEG)_x$-$(PCL)_y$ are presented in Figure 4. An intense and distinct peak at around 1724 cm^{-1} is due to the stretching frequency of the ester group C=O bond in the copolymers, which is not present in the pristine mPEG. The appearance of another intense and distinct peak at around 1110 cm^{-1} also confirmed the presence of the C-O bond in the copolymers. These two peaks can be used to indicate that the formation of the ester linkage between the copolymer and mPEG is successful during the esterification of the ring-opening reaction. Additionally, the peak at around 2946 cm^{-1} is due to the aliphatic C-H stretching of mPEG and the copolymers.

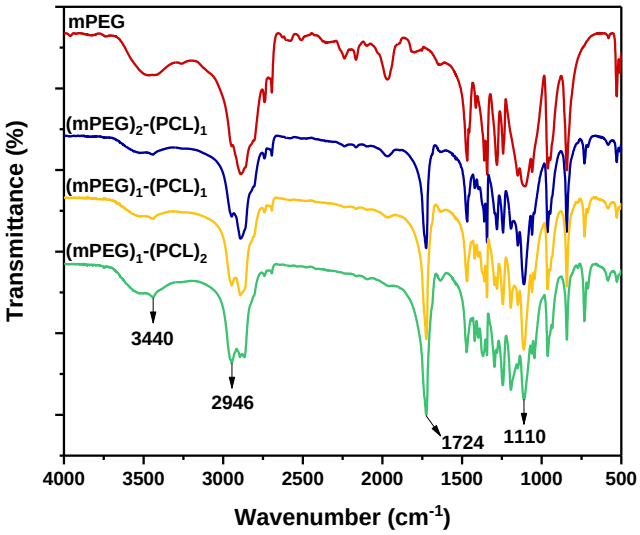

Fig. 4. FTIR spectra of mPEG, $(mPEG)_2$-$(PCL)_1$, $(mPEG)_1$-$(PCL)_1$ and $(mPEG)_1$-$(PCL)_2$.

Surface morphology of copolymers $(mPEG)_x$-$(PCL)_y$

The surface morphologies of mPEG and the different compositions for copolymers $(mPEG)_x$-$(PCL)_y$ are shown in Figure 5. In Figure 5b, it can be seen that $(mPEG)_2$-$(PCL)_1$ consists predominantly of mPEG due to its higher mass ratio while the compositions of mPEG and PCL are approximately even, as shown in Figure 5c. As the mass ratio of PCL increases, the surface morphology appeared much rougher and a network-like structure could be seen (Figure 5d), which suggests a higher extent of entanglement of the $(mPEG)_1$-$(PCL)_2$ copolymer.

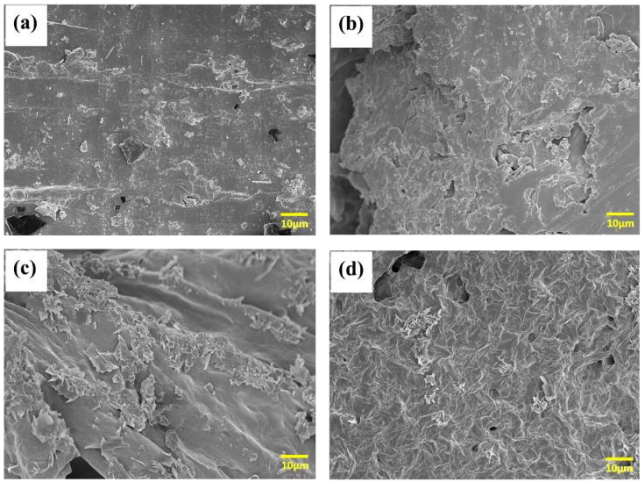

Fig. 5. SEM images of (a) mPEG, (b) $(mPEG)_2$-$(PCL)_1$, (c) $(mPEG)_1$-$(PCL)_1$, and (d) $(mPEG)_1$-$(PCL)_2$ copolymer.

TGA analysis

TGA was performed for pristine mPEG and all $(mPEG)_x$-$(PCL)_y$ copolymers to study their thermal stabilities as shown in Figure 6. From the TGA graph, it can be seen that pristine mPEG only has one decomposition step while all the $(mPEG)_x$-$(PCL)_y$ copolymers have two degradation steps. This could be supported by the derivative thermogravimetry (DTG) graphs that show only one peak for pristine mPEG and two or more peaks for all the $(mPEG)_x$-$(PCL)_y$ copolymers. Meanwhile, as seen in the TGA graph, the first degradation step of the $(mPEG)_x$-$(PCL)_y$ copolymers is due to the loss of PCL, which

increases with the increase of the weight percentage of PCL in the copolymer. This correlation could be verified by the DTG graph where the peak of the derivative weight change increases as the percentage of PCL increases. Likewise, the second degradation step seen in the TGA graph is due to the presence of mPEG which decreases as the average weighted amount of mPEG decreases in the copolymer and this could also be supported by the decreased derivative weight change percentage at the second peak of the copolymers at the DTG graph. Based on these results, the copolymers are thermally stable up to 150 °C and hence are suitable for TES applications.

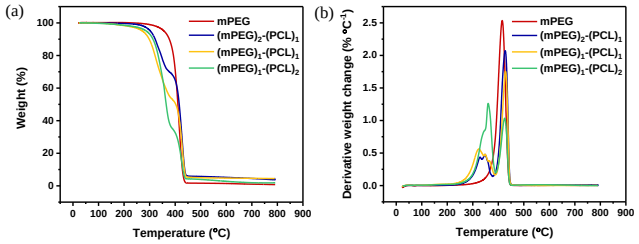

Fig. 6. (a) Thermogravimetry, and (b) derivative thermogravimetry curves of pristine mPEG and copolymers $(mPEG)_x$-$(PCL)_y$.

DSC analysis

The DSC curves of pristine mPEG and copolymers $(mPEG)_x$-$(PCL)_y$ and their thermal properties are shown in Figure 7. DSC analysis revealed that pristine mPEG has the highest melting temperature of 64.2 °C and latent heat of melting of 200.8 J g^{-1}. On the other hand, the $(mPEG)_x$-$(PCL)_y$ copolymers have a melting temperature and latent heat range of approximately 52.8-57.9 °C and 88.8-114.4 J g^{-1}, respectively. Understandingly, the decrease in latent heat from $(mPEG)_2$-$(PCL)_1$ to $(mPEG)_1$-$(PCL)_2$ is due to the increase in the mass ratio and average molecular weight of PCL, which has a theoretical melting enthalpy of 135 J g^{-1},[58] which is considerably lower than that of pristine mPEG. The theoretical melting enthalpy of the three copolymers was calculated based on the mass ratios of mPEG and PCL and they are shown in Table 3, together with the experimental melting enthalpy. The theoretical values are higher than the experimental melting enthalpy values and these imply that a fraction of mPEG is not crystallized. This is due to the interaction between mPEG and ε-caprolactone, resulting in a fraction of mPEG existing in the amorphous state. Nevertheless, it should be noted that the calculations of the theoretical melting enthalpy are only applicable to composites and therefore can only serve as a rough estimate since the copolymers were synthesized via chemical methods and the different bonding interactions should be considered.

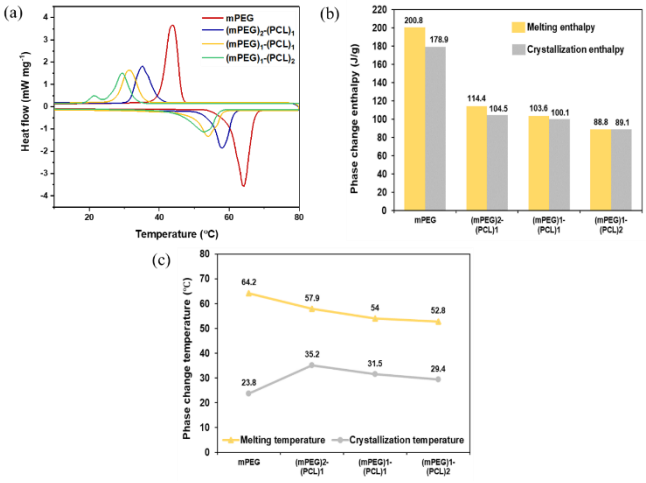

Fig. 7. (a) DSC curves, (b) phase change enthalpies, and (c) phase change temperatures of pristine mPEG and copolymers $(mPEG)_x$-$(PCL)_y$.

Table 3. Theoretical and experimental melting enthalpy of copolymers $(mPEG)_x$-$(PCL)_y$.

Sample	Theoretical melting enthalpy of mPEG (J/g)	Theoretical melting enthalpy of PCL (J/g)	Total theoretical melting enthalpy (J/g)	Experimental melting enthalpy (J/g)
$(mPEG)_2$-$(PCL)_1$	133.9	45.0	178.9	114.4
$(mPEG)_1$-$(PCL)_1$	100.4	67.5	167.9	103.6
$(mPEG)_1$-$(PCL)_2$	66.9	90.0	156.9	88.8

Form stability of copolymers $(mPEG)_x$-$(PCL)_y$

A leakage test for the copolymers $(mPEG)_2$-$(PCL)_1$, $(mPEG)_1$-$(PCL)_1$ and $(mPEG)_1$-$(PCL)_2$ was conducted at 75 °C, which is above the melting points of the copolymers, to evaluate the form-stable performance. Figure 8a depicts the digital photographs of the copolymers before and after the leakage test while Figure 8b shows the leakage rate of the copolymers. It was observed that the shape of all the $(mPEG)_x$-$(PCL)_y$ copolymers remained unchanged and no visible signs of leakage from the samples were detected as well. The leakage rate was calculated for the copolymers and the results attest to the preceding statement, with minimal and largely similar leakage (0.54% to 0.62%) for all three copolymers. This implies that mPEG moieties have been successfully grafted onto PCL, thus preventing their leakage and endowing the copolymers with excellent form stability.

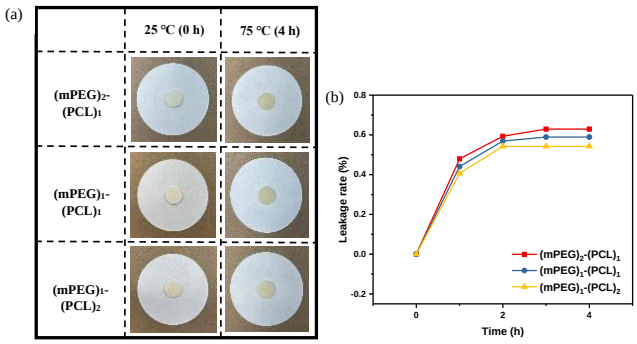

Fig. 8. (a) Photographs of the leakage test of copolymers $(mPEG)_x$-$(PCL)_y$ before and after heating to 75 °C for 4 h, and (b) The leakage rate (%) over time analysis plots.

Thermal cycling

Thermal reliability is an important factor for heat storage applications. Considering both the form stability and latent heat of all three copolymers, $(mPEG)_2$-$(PCL)_1$ was selected as the promising candidate for TES applications. To assess the thermal reliability of the copolymer, a thermal cycling of 100 cycles was carried out and the DSC curves and the analysis results after 0, 25, 50, 75, and 100 cycles are presented in Figure 9. The DSC curves remained unchanged and exhibited almost identical exothermic and endothermic peaks after 100 thermal cycles. Furthermore, the enthalpies and phase transition temperatures remained fairly constant, seemingly unaffected by the thermal cycling. This result indicated and confirmed the high thermal reliability of the copolymer.

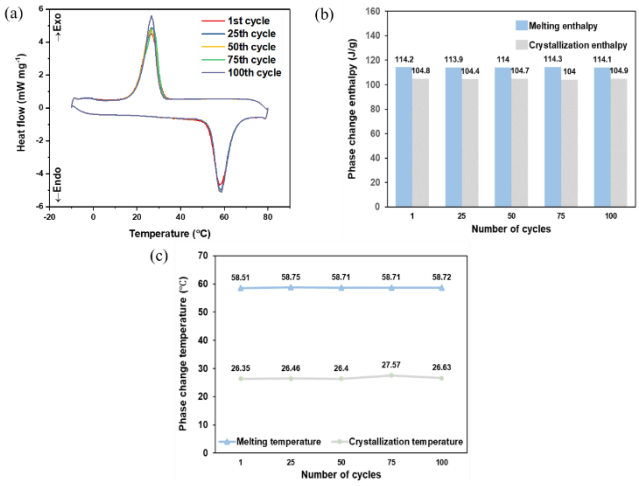

Fig. 9. (a) Thermal cycling DSC curves, (b) phase change enthalpies, and (c) phase change temperatures of $(mPEG)_2$-$(PCL)_1$ consisting of the 0^{th}, 25^{th}, 50^{th}, 75^{th}, and 100^{th} cycle.

TES performance test

Besides the aforementioned applications of $(mPEG)_x$-$(PCL)_y$ copolymers, a potential application is to use them as FSPCMs for TES applications. For example, they can be used in battery thermal management systems to regulate the battery temperature and ensure it is within the safe operating range. In thermoelectric applications,[59-60] the waste heat stored in these materials can be converted into useful electrical energy via a thermal gradient. In addition, these copolymers can be used for heating water storage tanks by wrapping them around the water pipes, whereby the heat stored during the day will be released at night when the ambient temperature falls. To demonstrate this particular application, $(mPEG)_2$-$(PCL)_1$ was shaped along a stainless-steel pipe as described in section 2.9, and the IR images and temperature readings are shown in Figure 10 and Table S1. Prior to the start of the experiment, the temperatures at the three different positions (P1, P2, and P3) are approximately 23.0 °C. After the water has been heated at 80 °C for 15 min to allow the copolymer to absorb the maximum amount of heat, P3 has the highest temperature of 59.1 °C due to the heat stored in the copolymer. P1 (58.9 °C) has a slightly higher temperature than P2 (58.7 °C) and this is attributed to minor heat loss from the water as it flowed along the pipe. After the water circulator has been set to 25 °C, the temperature at P1 remained higher than P2 during the cooling phase for up to 40 min. After 50 min, it was observed that P2 has a higher temperature than P1 and P3 has a temperature of 40.4 °C, which is in the phase transition temperature range of the copolymer during the cooling phase. As a result, the heat released during this phase transition was gained by the water flowing past the copolymer and subsequently resulted in a higher temperature at P2 compared to P1. This has shown that that there was not much delay in the phase transition of the copolymer and that the entire process was efficient. In this regard, the copolymer has shown its potential as a FSPCM to release stored heat gradually for prolonged heating applications as well as in a wider range of TES applications due to its good form stability.

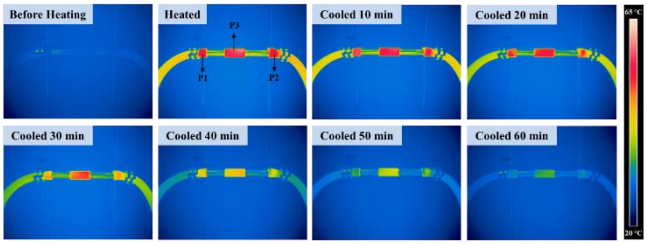

Fig. 10. IR images of TES application experiment at regular intervals.

Conclusion

In summary, a series of $(mPEG)_x$-$(PCL)_y$ copolymers with different mass percentages of mPEG were synthesized via ring-opening polymerization of ε-caprolactone with mPEG. These $(mPEG)_x$-$(PCL)_y$ copolymers were used as FSPCMs in which mPEG and PCL functioned as a PCM and a supporting material, respectively. DSC results showed that the copolymers have a melting temperature and latent heat range of 52.8-57.9 °C and 88.8-114.4 J g^{-1}, respectively, and TGA data revealed that they are thermally stable up to 150 °C. A leakage test that was conducted for the copolymers indicated minimal leakage of mPEG, which suggests that they have excellent form stability. $(mPEG)_2$-$(PCL)_1$, which was selected for further evaluation, exhibited good thermal reliability during thermal cycling. In addition, taking heating water storage tanks as an example, a TES application was carried out to investigate the performance of $(mPEG)_2$-$(PCL)_1$ as an energy storage material. During the experiment, this copolymer displayed excellent form stability and it was able to store and subsequently release heat when the heat source was removed, thus demonstrating its ability to absorb heat during the day and release it when the ambient temperature falls at night. Our results open up another potential application of $(mPEG)_x$-$(PCL)_y$ copolymers as FSPCMs for TES applications due to their excellent form stability and relatively high latent heat. mPEG with different molecular weights could be used to fine-tune the phase transition temperature of the copolymers to cater to different applications, while nano additives with high thermal conductivity such as metallic nanoparticles, graphene, or carbon nanotubes could be added as well to improve the thermal conductivity of mPEG.

Supporting Information Summary

Supporting Information includes a sample calculation for determining the degree of polymerization and the temperature readings for the TES performance test.

Acknowledgments

This work is supported by A*STAR Career Development Fund (Grant Number: C210812038).

Conflict of Interest

The authors declare no conflicts of interest.

Data Availability Statement

The data that support the findings of this study are available from the corresponding author upon reasonable request.

Keywords: energy conversion · phase change material · polycaprolactone · polyethylene glycol · polymers

References

[1] B. Lu, X. Meng, M. Zhu, R. O. Suzuki, *J. Electron. Mater.* **2018**, *47*, 3238-3247.
[2] X. Meng, R. O. Suzuki, *Appl. Therm. Eng.* **2016**, *99*, 352-357.
[3] M. Liu, J. Huang, H. Meng, C. Liu, Z. Chen, H. Yang, Z. Feng, X. Li, R. Luo, Z. Huang, *J. Eur. Ceram. Soc.* **2023**, *43*, 4198-4208.
[4] J. Wang, Z. Pan, Y. Wang, L. Wang, L. Su, D. Cuiuri, Y. Zhao, H. Li, *Addit. Manuf.* **2020**, *34*, 101240.
[5] P. Xu, Q. Yuan, W. Ji, R. Yu, F. Wang, N. Huo, *Mater. Express* **2022**, *12*, 1493-1501.
[6] T. Xin, S. Tang, F. Ji, L. Cui, B. He, X. Lin, X. Tian, H. Hou, Y. Zhao, M. Ferry, *Acta Mater.* **2022**, *239*, 118248.
[7] W. Kuang, H. Wang, X. Li, J. Zhang, Q. Zhou, Y. Zhao, *Acta Mater.* **2018**, *159*, 16-30.

[8] X. Fan, G. Wei, X. Lin, X. Wang, Z. Si, X. Zhang, Q. Shao, S. Mangin, E. Fullerton, L. Jiang, *Matter* **2020**, *2*, 1582-1593.
[9] P. J. Ong, Y. Y. Lum, X. Y. D. Soo, S. Wang, P. Wang, D. Chi, H. Liu, D. Kai, C.-L. K. Lee, Q. Yan, J. Xu, X. J. Loh, Q. Zhu, *Constr. Build. Mater.* **2023**, *386*, 131583.
[10] Z. M. Png, X. Y. D. Soo, M. H. Chua, P. J. Ong, J. Xu, Q. Zhu, *J. Mater. Chem. A* **2022**, *10*, 3633-3641.
[11] V. Bianco, M. De Rosa, K. Vafai, *Appl. Therm. Eng.* **2022**, *214*, 118839.
[12] M. Zhang, Y. Liu, S. F. Almojil, A. A. Rajhi, S. Alamri, A. I. Almohana, A. F. Alali, A. E. Anqi, Z. Tang, T. I. Kh, *J. Build. Eng.* **2022**, *57*, 104933.
[13] Q. Zhu, E. Yildirim, X. Wang, A. K. K. Kyaw, T. Tang, X. Y. D. Soo, Z. M. Wong, G. Wu, S.-W. Yang, J. Xu, *Mol. Syst. Des. Eng.* **2020**, *5*, 976-984.
[14] X. Yong, G. Wu, W. Shi, Z. M. Wong, T. Deng, Q. Zhu, X. Yang, J.-S. Wang, J. Xu, S.-W. Yang, *J. Mater. Chem. A* **2020**, *8*, 21852-21861.
[15] J. Zheng, S. F. D. Solco, C. J. E. Wong, S. A. Sia, X. Y. Tan, J. Cao, J. C. C. Yeo, W. Yan, Q. Zhu, Q. Yan, *J. Mater. Chem. A* **2022**, *10*, 19787-19796.
[16] V. Skurkyte-Papieviene, A. Abraitiene, A. Sankauskaite, V. Rubeziene, J. Baltusnikaite-Guzaitiene, *Polymers* **2021**, *13*, 1120.
[17] H. Ke, Y. Li, J. Wang, B. Peng, Y. Cai, Q. Wei, *Renew. Energy* **2016**, *99*, 1-9.
[18] S. Y. Kee, Y. Munusamy, K. S. Ong, *Appl. Therm. Eng.* **2018**, *131*, 455-471.
[19] D. Wu, B. Ni, Y. Liu, S. Chen, H. Zhang, *J. Mater. Chem. A* **2015**, *3*, 9645-9657.
[20] K. Chen, X. Yu, C. Tian, J. Wang, *Energy Convers. Manage.* **2014**, *77*, 13-21.
[21] R. Gulfam, P. Zhang, Z. Meng, *Appl. Energy* **2019**, *238*, 582-611.
[22] X. Y. Soo, J. K. Muiruri, J. C. Yeo, Z. M. Png, A. Sng, H. Xie, R. Ji, S. Wang, H. Liu, J. Xu, X. J. Loh, Q. Yan, Z. Li, Q. Zhu, *SmartMat* **2023**, e1188.
[23] X. Y. D. Soo, Z. M. Png, M. H. Chua, J. C. C. Yeo, P. J. Ong, S. Wang, X. Wang, A. Suwardi, J. Cao, Y. Chen, Q. Yan, X. J. Loh, J. Xu, Q. Zhu, *Mater. Today Adv.* **2022**, *14*, 100227.
[24] B. Masaaki, K. Nemoto, D. Otaki, T. Sasaki, M. Takeda, N. Yamada, *Int. J. Heat Mass Transfer* **2021**, *179*, 121731.
[25] Y. Zhang, Z. Jia, A. M. Hai, S. Zhang, B. Tang, *Compos. Part A: Appl. Sci. Manuf.* **2022**, 107047.
[26] Q. Sun, H. Zhang, Y. Yuan, X. Cao, L. Sun, *Adv. Eng. Mater.* **2018**, *20*, 1700643.
[27] X. Y. D. Soo, Z. M. Png, X. Wang, M. H. Chua, P. J. Ong, S. Wang, Z. Li, D. Chi, J. Xu, X. J. Loh, Q. Zhu, *ACS Appl. Polym. Mater.* **2022**, *4*, 2747-2756.
[28] P. J. Ong, Y. Leow, X. Y. D. Soo, M. H. Chua, X. Ni, A. Suwardi, C. K. I. Tan, R. Zheng, F. Wei, J. Xu, X. J. Loh, D. Kai, Q. Zhu, *Waste Manage.* **2023**, *157*, 339-347.
[29] K. Yu, Y. Liu, Y. Yang, *J Energy Storage* **2021**, *43*, 103172.
[30] K. Sun, Y. Kou, H. Zheng, X. Liu, Z. Tan, Q. Shi, *Sol. Energy Mater. Sol. Cells* **2018**, *178*, 139-145.
[31] J. Shi, M. Li, *Sol. Energy* **2020**, *205*, 62-73.
[32] C. Chen, W. Liu, Z. Wang, K. Peng, W. Pan, Q. Xie, *Sol. Energy Mater. Sol. Cells* **2015**, *134*, 80-88.
[33] W. Wu, W. Wu, S. Wang, *Appl. Energy* **2019**, *236*, 10-21.
[34] X. Zhu, L. Han, F. Yang, J. Jiang, X. Jia, *Sol. Energy Mater. Sol. Cells* **2020**, *208*, 110361.
[35] T. Wang, X. Qiu, X. Chen, L. Lu, B. Zhou, *Appl. Energy* **2022**, *325*, 119832.
[36] L. Kong, Y. Liu, L. Dong, L. Zhang, L. Qiao, W. Wang, H. You, *Dalton Trans.* **2020**, *49*, 1947-1954.
[37] J. Yang, L.-S. Tang, R.-Y. Bao, L. Bai, Z.-Y. Liu, B.-H. Xie, M.-B. Yang, W. Yang, *Sol. Energy Mater. Sol. Cells* **2018**, *174*, 56-64.
[38] Y. Fang, H. Kang, W. Wang, H. Liu, X. Gao, *Energy Convers. Manage.* **2010**, *51*, 2757-2761.
[39] S. Karaman, A. Karaipekli, A. Sarı, A. Bicer, *Sol. Energy Mater. Sol. Cells* **2011**, *95*, 1647-1653.
[40] Y. Yang, Y. Pang, Y. Liu, H. Guo, *Mater. Lett.* **2018**, *216*, 220-223.
[41] Z. Liu, Y. Zhang, K. Hu, Y. Xiao, J. Wang, C. Zhou, J. Lei, *Energy Build.* **2016**, *127*, 327-336.
[42] G. Alva, Y. Lin, G. Fang, *Sol. Energy Mater. Sol. Cells* **2018**, *186*, 14-28.
[43] W. Kong, Y. Lei, Y. Jiang, J. Lei, *J. Therm. Anal. Calorim.* **2017**, *130*, 1011-1019.

[44] Y. Tan, Y. Xiao, R. Chen, C. Zhou, L. Wang, Y. Liu, D. Li, *Chem. Eng. J.* **2020**, *396*, 125265.
[45] P.-B. Chen, J.-W. Yang, Z.-X. Rao, Q. Wang, H.-T. Tang, Y.-M. Pan, Y. Liang, *J. Colloid Interface Sci.* **2023**.
[46] S. Yin, X. Ren, R. Zheng, Y. Li, J. Zhao, D. Xie, Y. Mei, *Chem. Eng. J.* **2023**, *464*, 142683.
[47] H. Jiang, Y. Xie, R. Zhu, Y. Luo, X. Sheng, D. Xie, Y. Mei, *Chem. Eng. J.* **2023**, *456*, 141049.
[48] E. Malikmammadov, T. E. Tanir, A. Kiziltay, V. Hasirci, N. Hasirci, *J. Biomater. Sci. Polym. Ed.* **2018**, *29*, 863-893.
[49] X. J. Loh, W. Guerin, S. M. Guillaume, *J. Mater. Chem.* **2012**, *22*, 21249-21256.
[50] J. J. C. Lee, S. Sugiarto, P. J. Ong, X. Y. D. Soo, X. Ni, P. Luo, Y. Y. K. Hnin, J. S. Y. See, F. Wei, R. Zheng, P. Wang, J. Xu, X. J. Loh, D. Kai, Q. Zhu, *J Energy Storage* **2022**, *56*, 106118.
[51] L. Jiang, J. Zhang, in *Applied Plastics Engineering Handbook (Second Edition)* (Ed.: M. Kutz), William Andrew Publishing, **2017**, pp. 127-143.
[52] K. Wu, L. Yu, J. Ding, *J. Chem. Educ.* **2020**, *97*, 4158-4165.
[53] X. J. Loh, B. J. H. Yee, F. S. Chia, *J. Biomed. Mater. Res. A* **2012**, *100*, 2686-2694.
[54] M. R. Dethe, A. Prabakaran, H. Ahmed, M. Agrawal, U. Roy, A. Alexander, *J. Controlled Release* **2022**.
[55] F. Lu, L. Lei, Y.-Y. Shen, J.-W. Hou, W.-L. Chen, Y.-G. Li, S.-R. Guo, *Int. J. Pharm.* **2011**, *419*, 77-84.
[56] A. Behl, V. S. Parmar, S. Malhotra, A. K. Chhillar, *Polymer* **2020**, *207*, 122901.
[57] W. Peng, X.-y. Jiang, Y. Zhu, E. Omari-Siaw, W.-w. Deng, J.-n. Yu, X.-m. Xu, W.-m. Zhang, *Acta Pharmacologica Sinica* **2015**, *36*, 139-148.
[58] S. Nakagawa, K.-i. Kadena, T. Ishizone, S. Nojima, T. Shimizu, K. Yamaguchi, S. Nakahama, *Macromolecules* **2012**, *45*, 1892-1900.
[59] T. Tang, A. K. K. Kyaw, Q. Zhu, J. Xu, *Chem. Commun.* **2020**, *56*, 9388-9391.
[60] J. Cao, Y. Sim, X. Y. Tan, J. Zheng, S. W. Chien, N. Jia, K. Chen, Y. B. Tay, J. F. Dong, L. Yang, *Adv. Mater.* **2022**, *34*, 2110518.

Table of Contents

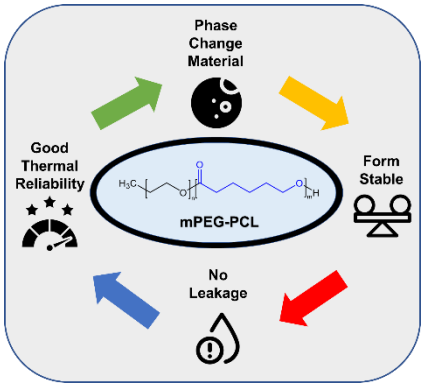

This work reports the synthesis of a series of monomethoxy poly(ethylene glycol)-polycaprolactone (mPEG-PCL) copolymers with different mass percentages of mPEG as form-stable phase change materials for thermal energy storage (TES) applications. Excellent form stability was exhibited by the copolymers and the ability to store and release heat for a prolonged period was demonstrated as well.